Energy Demand for Pyrolysis of Mixed Thermoplastics and Waste Plastics in Chemical Recycling: Model Prediction and Pilot-Scale Validation

Niklas Netsch,* Michael Zeller, Frank Richter, Britta Bergfeldt, Salar Tavakkol,* and Dieter Stapf

ABSTRACT: Pyrolysis of plastic waste is a key technology for closing the anthropogenic carbon cycle. The energy demand (ED) of this endothermic process is a crucial factor to evaluate its benefits compared to established recycling pathways. The pyrolysis ED can be determined experimentally. However, this is elaborate and limited in transferability. Existing models cover virgin plastics or hydrocarbon thermoplastic mixtures on a laboratory scale. Here, a model for calculating the ED of thermoplastic mixtures based on the superposition of virgin polymer data is developed. The material data, such as heat capacity, phase transition enthalpy, and reaction enthalpy, are determined using differential scanning calorimetry. Pilot-scale experiments are performed in a 1 kg/h screw reactor. These experimental data are compared to model calculations. The feedstock-specific ED for pyrolysis is plastic-type independent. It amounts to approximately 4−6% of the feedstocks' net calorific value. The validation shows excellent accordance for virgin plastics and hydrocarbon plastics mixtures. The modeled ED of mixtures including heteroatoms is systematically underestimated, which indicates changes in the degradation mechanism. The model allows for resolving several phenomena contributing to the pyrolysis ED. The simple calculation of the ED with in-depth information on occurring phenomena enables more reliable process design, optimization, and evaluation.

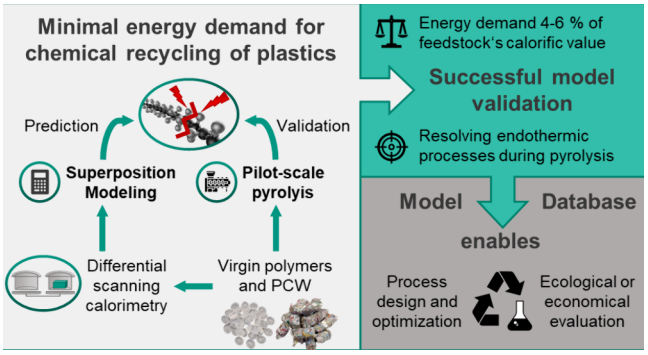

KEYWORDS: *plastic recycling, chemical recycling, pyrolysis, energy demand, thermal degradation, polymer decomposition, differential scanning calorimetry*

INTRODUCTION

The transition from linear value chains to a circular carbon economy is a key element of climate neutrality.[1] Herein high-calorific waste plastics can substitute fossil feedstocks, e.g., naphtha, in chemical synthesis.[2] Different recycling technologies are considered to accomplish the recycling targets of industrialized nations.[3−7] Complementary to mechanical recycling, various solvent-based and thermochemical processes are considered as chemical recycling options, often highlighting pyrolysis technologies as they recycle mixed plastic wastes to virgin polymers via the naphtha steam-cracking route.[8]

When the pyrolysis process is evaluated compared to existing waste treatment routes, the product yield and energy demand (ED) are crucial factors for cost estimations and assessments of potential environmental benefits of the endothermic pyrolytic process.[9] Because the thermal decomposition mechanism of plastic waste highly depends on the feedstock composition, the ED must be obtained experimentally. Numerous studies have used differential scanning calorimetry (DSC) to determine the pyrolysis ED for various polymers on a laboratory scale.[10−15] As shown in Table 1, the energy needed for pyrolysis strongly depends on the polymer type and the evaluation methodology.

Most plastic waste considered for chemical recycling features a heterogeneous composition. This limits investigations on a laboratory scale, which is why elaborate measurements on a pilot-plant scale are required to obtain reliable data. Zeller et al. report an estimation for the ED of about 5% of the pyrolyzed feedstock's net calorific value, being in a range of 23−34 kJ/g.[16] This ED is 2−5 times higher than the virgin polymer results for thermal decomposition shown in Table 1. This difference can be explained by the summation of the endothermic processes occurring during pyrolysis.[16] However, such EDs representing a global value for the heating of solid plastics, followed by melting, heating of the plastic melt until

Table 1. Pyrolysis Energy Demand of Different Polymer Types Differentiated According to Endothermic Processes via DSC

polymer type	physical or chemical phenomena	energy demand (J/g)	ref
PE	melting	75	12
		97	11
		218	15
	thermal decomposition	299	12
		365–575	10
		665	13
		920	15
		975	11
		1375	14
PP	melting	66	11
		80	15
	thermal decomposition	339–616	10
		632	13
		944	11
		1310	15
PS	thermal decomposition	690–732	10
		820	13
		855	11
		1000	15
ABS	thermal decomposition	647	11
PET	melting	35	11
		37	15
	thermal decomposition	217	11
		1800	15
PA6	thermal decomposition	787	13
PVC	thermal decomposition	170 (1st step), 540 (2nd step)	15

thermal decomposition, and product evaporation, prevent the differentiation of dominant endothermic phenomena. However, knowledge about the endothermic processes is fundamental to optimizing pyrolysis processes toward lower energy consumption. Cafiero et al. and Straka et al. present models for ED calculation assuming the superposition of individual components.[11,17] Nevertheless, these studies only cover polyolefins like polyethylene (PE) and polypropylene (PP) or polystyrene (PS), acrylonitrile butadiene styrene (ABS), and poly(ethylene terephthalate) (PET). Other important polymers of important waste streams,[18] e.g., polyamide 6 (PA6) or poly(vinyl chloride) (PVC), are not investigated. Validations on a pilot scale are only performed to a limited extent.

Therefore, a data-driven model for predicting the ED for mixtures of low-density PE (LDPE), high-density PE (HDPE), PP, PS, ABS, PET, PA6, and PVC is presented. The model is based on the linear superposition of virgin polymer material data. Individual endothermic steps, namely, sensible heat of different phases, melting, pyrolytic reaction, and product evaporation, are resolved. To validate the model results, pilot-scale experiments are conducted for exemplary thermoplastics, thermoplastic mixtures, and post-consumer waste (PCW).

MATERIALS AND METHODS

Polymeric Feedstock. Different thermoplastics, namely, Hostalen ACP 9255 Plus (HDPE), Lupolen 24020H (LDPE), Moplen HP 552H (PP), Styrolution 156F (PS), Sinkral F332 (ABS), and Alphalon 27 (PA6), were used. PET was supplied by Plastikpak Italia Preforme. These polymers were acquired as white or transparent primary granules with a particle size of 2–5 mm. They are free of additives, such as inorganic fillers, UV stabilizers, colorants, or flame retardants. In pilot-scale tests, a PVC granulate manufactured by Inovyn was used. It contains approximately 10 wt % inorganic fillers ($CaCO_3$ and TiO_2), as well as 2–3 mol % stabilizers. An additive-free PVC powder, Primex P225-2 (virgin PVC), was investigated in DSC. The polymers were analyzed for their elemental composition, moisture, ash content, and higher heating value (HHV). Carbon, hydrogen, and nitrogen were determined according to DIN EN 15104 with a LECO elemental analyzer (Truspec CHN Micro). Chlorine was analyzed after combustion via ion chromatography according to DIN EN 14582 (AQF-2100 Combustion IC including an Aquion IC) from a1-environsciences GmbH and Thermo Fisher Scientific GmbH. The detection limit of the chlorine measurement is 30 ppm. The analytical results including the lower heating value (LHV), which was calculated via the Boie formula from elemental analysis are shown in Table 2. Except for PCW, the HHV of the PVC-containing feedstocks was not determined experimentally due to potential corrosion.

Table 2. Elemental Composition, Moisture, Ash Content, and Calculated and Experimentally Determined Heating Values of the Investigated Feedstocks

	composition (m.%)							heating value (MJ/kg)		
polymer	C	H	N	Cl	moisture	ash	O[a]	LHV[b]	HHV[b]	HHV[c]
LDPE	85.8	14.2	<0.3	0.0	<0.01	<0.01	0.0	43.2	46.3	46.3
HDPE	85.8	14.2	<0.3	0.0	<0.01	<0.01	0.0	43.2	46.3	46.1
PP	85.8	14.2	<0.3	0.0	<0.01	<0.01	0.0	43.2	46.3	46.1
PS	92.0	8.0	<0.3	0.0	<0.01	<0.01	0.0	39.5	41.3	41.3
ABS	86.2	8.0	5.5	0.0	0.33	<0.01	0.0	37.9	39.6	39.6
PET	63.3	4.4	<0.3	0.0	0.19	<0.01	32.1	22.7	23.7	22.9
PA6	63.6	9.8	12.6	0.0	1.24	<0.01	12.7	30.8	33.0	31.2
PVC granulate	36.2	4.9	<0.3	47.9	0.16	10.6	0.3	17.2	18.3	
virgin PVC	39.6	5.6	<0.3	54.7	0.1	<0.01	0.0	19.0	20.3	
Mix 1[d]	87.6	12.4	0.0	0.0	0.0	0.0	0.0	42.1	44.8	
Mix 2[d]	83.5	13.4	0.3	1.0	0.0	0.2	1.6	41.5	44.5	
Mix 3[d]	84.5	13.6	0.3	0.0	0.0	0.0	1.6	42.0	45.0	
Mix 4[d]	80.6	11.6	0.9	2.4	0.1	0.5	3.9	38.6	41.1	
PCW	80.0	12.3	0.8	1.4	0.0	2.2	3.2	39.1	41.2	41.8

[a]Calculated as a difference to 100 mol %. [b]Calculated from elemental analysis. [c]Determined experimentally. [d]Calculated from a proportion of individual polymers in the mixture.

Four different mixtures of thermoplastics were prepared to validate the model on a pilot scale. These model mixtures represent thermoplastics-rich fractions of lightweight packaging waste of different quality. A simple mixture (Mix 1) of LDPE, PP, and PS was pyrolyzed. A more complex polyolefin-rich model mixture (Mix 2) consisted of nitrogen-, oxygen-, and chlorine-containing polymers. A similar mixture with reduced chlorine content (Mix 3) was also investigated. A fourth thermoplastic mixture with higher nitrogen, oxygen, and chlorine contents (Mix 4) was employed. After the polymers were weighed, the mixtures were homogenized by intensive manual mixing before being added to the feedstock hopper of the pyrolysis reactor. Additionally, PCW was pyrolyzed to evaluate the transferability of the additive-free model to functionalized plastic waste. This waste results from a collection of end-of-life packaging and consumer products with defined labeling according to the European identification system for packaging materials.[19] The waste was washed and dried to avoid moisture or biomass contaminations. Stick-on labels were removed. Further pretreatment included a two-stage shredding (Untha RS30 and Retsch SM-2000) and subsequent pelletizing (Amandus Kahl Type 14-175) to cylindrical pellets of 6 mm diameter and 5−15 mm height. During the preparation steps, the PCW is mixed manually to promote additional homogenization of the PCW pellets. The respective material data are also listed in Table 2. The data of the model mixtures are calculated from the pure substances. Table 3 displays the detailed composition of the thermoplastic mixtures.

Laboratory-Scale Experiments. The material properties were determined using DSC for all polymers. The enthalpy of fusion and pyrolysis enthalpy were experimentally determined in a Netzsch 214 Polyma differential scanning calorimeter. Approximately 10 mg of material was weighed in aluminum crucibles with pierced lids. The samples were heated and cooled twice in a nitrogen atmosphere from 30 to 300 °C, for PVC up to 200 °C, with a heating rate of 10 K/min. The temperature program was chosen to ensure that no significant decomposition reactions occurred during the first heating phase. In the second heating cycle, the temperature was increased to 550 °C for determining the pyrolysis reaction enthalpy. Every polymer was measured twice, and the results were averaged. The heat capacity of the plastics and sand used in the pilot-scale tests was determined on a Netzsch DSC 204 F1 in an argon atmosphere with a heating rate of 10 K/min in the temperature range from −20 to +300 °C. The DSC calibration was carried out with indium, zinc, tin, bismuth, and lead according to DIN 51007.[20] The heat capacity was determined using the sapphire method, conforming to the DIN 51007 standard. By including the melting, glass transition (GT), and pyrolysis temperatures, the heat capacity of the various plastics can be derived. The temperatures are determined from characteristic points in the DSC curves according to DIN ISO 11357.[21] The melting peak temperature in the DSC curve and the temperature associated with the inflection point of the GT are applied. Based on the DSC data, three options exist for determining the reaction temperature. These options open a potential range for the parameter choice.

Table 3. Composition of the Thermoplastic Mixtures Applied in Pilot-Scale Pyrolysis Experiments

	share of polymer in the model and PCW mixture (m.%)				
polymer	Mix 1	Mix 2	Mix 3	Mix 4	PCW
LDPE	40.0	70.0	71.96	50.0	29.4
HDPE					17.1
PP	30.0	20.0	20.0	15.0	25.1
PS	30.0	2.0	2.0	10.0	4.2
ABS				5.0	3.8
PET		4.0	4.0	10.0	10.1
PA6		2.0	2.0	5.0	6.3
PVC		2.0	0.04	5.0	4.0

First, the initial start of the polymer decomposition may be applied, which can be referred as the onset temperature of the reaction. Second, the peak temperature of the reaction can be selected. This parameter reflects the temperature with the highest reaction rate in DSC. Last, the temperature at which full conversion is reached may be used. This temperature reflects the temperature at which the DSC curve meets the baseline again and full conversion is reached. The selection of the reaction temperature is investigated in more detail in a sensitivity study (see the Supporting Information). The onset temperature is about 20 K lower than the DSC peak point used in this study, while the temperature of full conversion is about 20−30 K higher than the temperature used in the paper. The polymer is already decomposing during heating to the reactor temperature in the experiments. Using the onset temperature neglects further heating of unreacted molecules at higher temperatures during this heating process, therefore, it has not been chosen. In turn, implementing the temperature of full conversion in thermogravimetric analysis (TGA) would reflect additional heating of already decomposed molecules in the modeling. This selection increases the ED. Consequently, both options lead to a higher deviation from the real process. The enthalpy of the reaction, determined as the calibrated area under the DSC curve, remains unaffected. The values calculated with peak temperatures from DSC reflect an average value within this interval. Therefore, the DSC peak temperature selection appears to be a reasonable, average choice in the temperature parameter range to define the reaction temperature in the model as it represents a mean value between the three options.[21]

Between the characteristic temperatures, the heat capacity is linearly approximated as a function of the temperature. A linear baseline is used to calculate the enthalpy of fusion following DIN 11357.[21] The baseline for determining the enthalpy required for polymer degradation and evaporation of the resulting products can be obtained in several ways.[10,22] When a Bézier curve baseline was applied, an average value between those of the tangential and linear methods was determined.

Pilot-Scale Experiments. Pilot-scale experiments were carried out using an electrically heated screw reactor. The experimental setup and procedure are described in detail by Zeller et al. and Netsch et al. for the pyrolysis of contaminated plastic waste and polyolefin-rich plastic mixtures.[16,23,24] The mass balance and ED were derived. The reactor temperature was set to 500 °C. This is necessary for the complete conversion of the polymer within the specified solid residence time of 30 min. To maximize the yield of condensable products, higher reactor temperatures are not desirable because they lead to increased gas formation. The reactor was operated with a feedstock input of 1 kg/h in a nitrogen atmosphere (12 L/min). Quartz sand was applied as the carrier material with a mass flow rate of approximately 4 kg/h. Feedstock and sand mass flow were determined before each test run since differences in the bulk density lead to deviations during material dosing. An ABB three-phase energy meter (type A43 313-100) recorded the electrical energy uptake of the reactor at 5 min intervals. The energy consumption of auxiliary equipment, including the condensation unit and the measurement and control unit, was counted separately. Startup and shutdown processes during the 5 h test runs were neglected so that approximately 3.5−4 h of continuous operation are included in the calculation of the ED. Each test was performed twice, and the determined values were averaged. Six experiments were conducted for Mix 2 to check reproducibility. Comparative experiments without feedstock addition were carried out for energy balancing, determining the required electrical energy consumption for sand and flush gas heating. The linearization of this basic ED depending on the supplied sand mass rate allowed flexible background demand adaption within the operating parameter window. Based on the energy difference of tests with and without feedstock, the feedstock-specific ED was calculated. The influence of the temperature, sand mass, and purge gas flow on the heat losses of the system was tested. Further information on the reactor setup can be found in the Supporting Information.

THEORETICAL CALCULATIONS

The model determines the mass-specific ED based on a superposition approach. As proposed by Cafiero et al. and Netsch et al., this approach neglects any interaction of the polymers during thermal degradation.[11,25] Reactor-specific heat losses are excluded, so calculated values represent the lower limit of the ED for the overall pyrolysis process. This minimal pyrolysis ED h_{py} of the entire pyrolysis process is calculated according to the mass fraction of each polymer in the mixture x_i following eq 1. The energy needed for solid polymer heating h_{solid} and for molten polymer heating h_{melt} is considered. Additionally, the equation comprises the feedstock-specific enthalpy of fusion h_f and the reaction enthalpy h_R, which includes the energy expended for product evaporation.

$$h_{py} = \sum_i x_i(h_{solid,i} + h_{f,i} + h_{melt,i} + h_{R,i}) \quad (1)$$

Initially, the energy for heating from ambient temperature T_a to the GT temperature T_g of the respective polymer i is calculated. In this temperature range, the specific heat capacity before GT $c_{p,preGT}$ is used. Between the state of GT and melting temperature T_m and from melting to reaction temperature T_R, the calculation is carried out analogously. The reaction temperature is defined as the degradation peak temperature. The sensible heat of the different heating stages is calculated according to eqs 2 and 3. The specific heat capacities before melting, $c_{p,postGT}$, and after melting, $c_{p,m}$, are also incorporated.

$$h_{f,i} = \int_{T_a}^{T_{g,i}} c_{p,preGT,i}\, dT + \int_{T_{g,i}}^{T_{m,i}} c_{p,postGT,i}\, dT \quad (2)$$

$$h_{R,i} = \int_{T_{m,i}}^{T_{R,i}} c_{p,m,i}\, dT \quad (3)$$

To linearize the temperature-dependent heat capacity, the DSC data are fitted following eq 4. The heat capacity for each polymer i in phase state j depends on the temperature T (°C) and the fit parameters A and B.

$$c_{p,j,i} = A_{i,j}T + B_{i,j} \quad (4)$$

Consequently, eqs 2 and 3 can be simplified by averaging the linearized heat capacities in the relevant temperature range, leading to eqs 5 and 6.

$$h_{solid,i} = \overline{c}_{p,preGT,i}(T_{g,i} - T_a) + \overline{c}_{p,postGT,i}(T_{m,i} - T_{g,i}) \quad (5)$$

$$h_{melt,i} = \overline{c}_{p,m,i}(T_{R,i} - T_{m,i}) \quad (6)$$

The enthalpy of phase transition is polymer-dependent. Thus, some terms are omitted for certain polymers. LDPE, HDPE, and PP show no GT in the relevant temperature range. In this case, eq 5 only consists of the postGT term while the preGT term is neglected. For PA6, a low GT temperature of about 50 °C is observed. The GT of PA6 is neglected, and only a postGT linearization of the specific heat capacity is considered from room temperature upward. ABS and PS lack a melting transition. Thus, the terms for sensible heat of ABS and PS melt, and their enthalpy of fusion are not considered. To linearize the heating process for different regimes, notional model limit temperatures for the different phases T^*_g and T^*_m are introduced. Those limit temperatures differ from the experimentally determined characteristic polymer temperatures. The integrated values for heat of fusion and the reaction enthalpy rely on a baseline similar to the linearized heat capacities. Therefore, the notional limit temperatures reflect the intersection of the linearized heat capacities. The method for defining the model limit temperatures and deriving the linearized heat capacities is depicted for PET in Figure 1. The determination method of the melting and reaction enthalpy for PET is shown in Figure 2.

RESULTS AND DISCUSSION

Laboratory Experiments. With this study, heat capacities can be determined as a function of temperature for all polymers except PVC in the range of 50−300 °C. Table 3 presents the determined characteristic material data. Also, the linearized heat capacities and the model limit temperatures are shown. The GT and melt temperatures, heat of fusion, and heat capacities are consistent with the available literature data.[26] In some cases, the resulting limit temperatures used as model parameters deviate from the calculated DSC values to meet heat capacity intersections. For example, the melting transition for PET and PA6 is selected about 80 °C before the determined peak temperature. For LDPE, HDPE, and PP, the model limit temperature of the melting transition is about 10−20 K higher than their peak melting temperature. The use of these model parameters allows a closer replication of the linearized heat capacities because their intersection point reflects the baseline for determination of the heat of fusion more accurately. The two-stage decomposition mechanism of PVC hinders the determination of all material values. Up to approximately 180 °C, reproducible data for heat capacity is obtained. The degradation start of PVC prevents determination of the heat capacity above 180 °C and also integration of the reaction enthalpy. The heat capacity is therefore assumed to be constant (2000 J/g·K) from 180 °C onward. Following Stoliarov and Walters, the enthalpy of the reaction for the multistage PVC mechanism is estimated to be 700 J/g·K.[15]

The determined reaction temperature is compared to the results of TGA.[25] This comparison indicates close consistency between the peak temperature of the DSC and the peak temperature of the differential thermogravimetric curve of only a few Kelvin (see the Supporting Information).

The heat capacity of the quartz sand $c_{p,Sand}$ (in J/kg·K) used in pilot-scale tests can be approximated based on the DSC results in the temperature range of 0−500 °C according to eq 7. Additionally, eq 8 represents an approximation to material data from the VDI heat atlas for calculating the heat capacity of

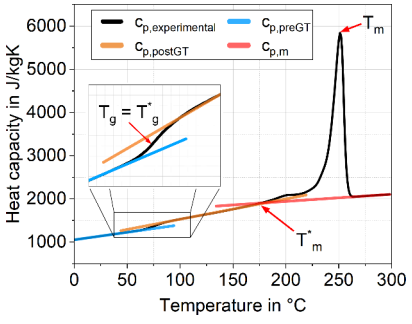

Figure 1. DSC data of PET marked with characteristic polymer temperatures (GT temperature T_g and melting temperature T_m), model limit temperatures (T_g* and T_m*), and linearized heat capacities before GT (blue), after GT (orange), and after melting (red).

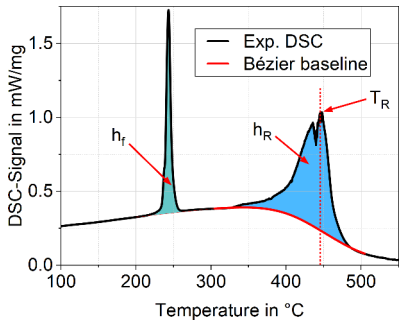

Figure 2. Integration of h_f and h_R and determination of T_R from the DSC data of PET with a Bézier baseline.

nitrogen from 0 to 600 °C.[27] The implementation is needed to match the model data to the experimental investigations in pilot scale.

$$c_{p,Sand} = 7 \times 10^{-12}T^5 - 8 \times 10^{-9}T^4 + 5 \times 10^{-6}T^3 - 0.0034T^2 + 1.8812T + 691.45 \quad (7)$$

$$c_{p,N_2} = 2 \times 10^{-15}T^5 - 3 \times 10^{-12}T^4 + 2 \times 10^{-9}T^3 + 7 \times 10^{-8}T^2 + 2 \times 10^{-6}T + 1.041 \quad (8)$$

The ED for thermal decomposition and melting of the polymers corresponds to the literature data summarized in Table 1. Because of the lower degree of crystallinity, the ED of the LDPE measured exhibits a lower heat of fusion than the HDPE, while both are in the range of the reported literature.[12,15] The DSC data of PP and PET reveal slightly higher heat of fusion than those reported by Cafiero et al. and Stoliarov et al.[11,15] The deviations may be caused by a different polymer configuration (e.g., degree of polymerization or additives). The measured ED for thermal decomposition of the polymers in this work, shown in Table 4, varies depending on the polymer type, as is evident for PE, PP, PS, and PET, for example. These results represent an average value in the stated range from the literature values in Table 4. Fewer comparative values are available for ABS and PA6. Still, the determined values are comparable, considering the influence of the evaluation methodology and differences in the structure and composition of the reported and used polymers.

Pilot-Scale Experiments. Pilot-scale pyrolysis experiments were carried out with pure LDPE, PP, PS, Mixes 1−4, and PCW to provide mass and energy balances. The mass balance for each feedstock is shown in Figure 3. The product fractions deviate by max. 2 m.%, and a minor balance loss of max. 3.9 m.% for Mix 2 indicates a high reproducibility. The mass balances depend on the selected feedstocks. Generally, the pyrolysis gas and the condensates dominate the product yields. Increasing amounts of heteroatom-containing polymer mixtures such as PET and PVC lead to the formation of a solid residue. The residue reaches up to 4.3 and 4.1 m.% for additive-containing PCW and heteroatom-containing Mix 4, respectively.

Figure 4 shows the plastic-related ED for the pyrolysis at 500 °C. This universal plastic-specific ED excludes the sand's reactor-specific contribution as a carrier material. It ranges from 1575 to 2424 J/g of added feedstock. However, the energy required for heating the sand to a reactor temperature of 500 °C is also determined experimentally in pilot scale. It accounts for approximately 460−490 J/g_{Sand}. The ED for sand heating modeled based on the DSC results is 471 J/g_{Sand} according to formula (7). Detailed results, including the carrier material contribution, are summarized in the Supporting information. The energy balance also shows clear feedstock-dependent variations. Pyrolyzing PS requires a significantly lower ED compared to polyolefins. A mixture of LDPE, PP, and PS (Mix 1) exhibits an ED between the determined pure polymer values. Mix 2, Mix 3, and Mix 4 show significantly higher ED than Mix 1. The higher ED may result from the more complex composition incorporating heteroatom-containing polymers like PA6, PET, or PVC. For such thermoplastic blends, Netsch et al. report significant polymer interactions during pyrolysis.[24] These interactions lead to differing degradation mechanisms, which could explain the discrepancies between the model and experimentally determined ED. PCW features a lower ED compared to the polymer mixtures. This may be attributed to the additive content because inert fillers and other nonpyrolyzable components reduce the ED of PCW or have a catalytic effect. Another possible reason for these deviating results is secondary reactions of volatile products in the gas phase. The screw reactor exhibits longer gas residence times in the heated zone compared to DSC experiments with a virgin polymer. Consequently, additional secondary gas phase reactions may occur, leading to changes in the reaction mechanism and product distribution. This may also influence the measured ED.

The feedstock and sand dosage fluctuate depending on the conveying behavior. Therefore, the dosing rate represents the main influencing factor for deviating results of repeated experiments. Also, polymer experiments slightly lower the

Table 4. Model Data for Calculation of the ED of Phase Transition, Polymer Heating, and Pyrolytic Degradation Including Evaporation Experimentally Determined via DSC

	phase transition			degradation reaction		linearized heat capacities A (J/g·K²) and B (J/g·K)			limit temperatures for modeling	
polymer	T_g (°C)	T_m (°C)	h_f (J/g)	T_R (°C)	h_R (J/g)	$c_{p,preGT}$	$c_{p,postGT}$	$c_{p,m}$	T^*_g (°C)	T^*_m (°C)
LDPE		112	142	478	473		A = 4.376, B = 2106	A = 3.336, B = 2238		125
HDPE		136	235	482	438		A = 6.447, B = 1674	A = 3.250, B = 2191		156
PP		164	116	459	542		A = 5.992, B = 1636	A = 3.095, B = 2161		180
PS	102			419	744	A = 5.308, B = 1207	A = 2.762, B = 1668		100	
ABS	109			422	739	A = 3.695, B = 1359	A = 2.454, B = 1796		105	
PET	73	251	56	443	232	A = 3.468, B = 1058	A = 4.719, B = 1061	A = 1.659, B = 1615	73	175
PA6		222	72	455	630		A = 9.241, B = 1368	A = 2.424, B = 2444		145
virgin PVC	87			256 (1st step), 470 (2nd step)		A = 3.290, B = 890	A = 5.415, B = 988	A = 0, B = 2000	87	180

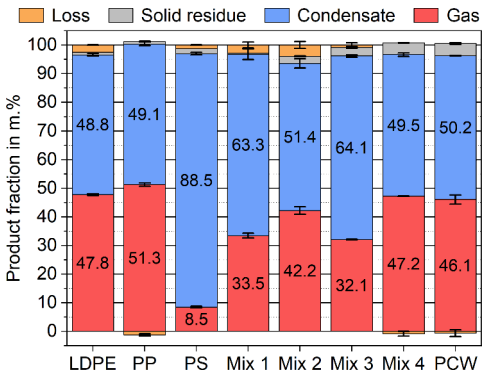

Figure 3. Average mass balance including standard deviation error bars of pilot-scale pyrolysis experiments at 500 °C with a feedstock dosing of 1 kg/h and a dwell time of 30 min.

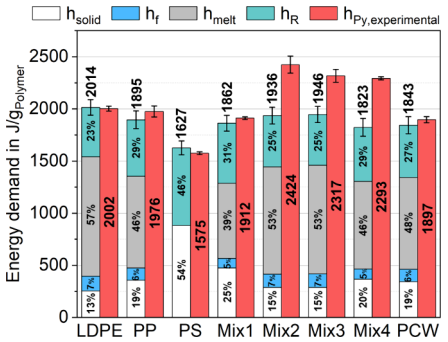

Figure 4. ED of the experimental measurements (red) and model calculations with subdivisions of heating of a solid polymer (white), heat of fusion (blue), heating of a polymer melt (grey), and reaction and product evaporation enthalpy (green).

reactor inlet temperature compared to the background measurement obtained with sand. This lower inlet temperature of up to 5 K reduces the heat emission to the environment, which is not compensable by background deduction. Nevertheless, the standard deviation of the ED for plastic pyrolysis accounts for only up to 81 J/g. Reducing the amount of sand as the carrier material favors the total ED of the pyrolysis process by minimizing the background ED.

Model Calculations. The model calculations are compared to the experimentally determined ED in Figure 4. The ED of the LDPE, PP, PS, and Mix 1 pyrolysis agrees with the model value within the range of measurement and model uncertainties. Different methods for selecting the reaction temperature influence the model results by less than 100 J/$g_{Polymer}$. For these feedstocks, the modeled ED for the pyrolysis deviates by less than about 5% of the experimental value. The results obtained with the more complex Mix 2, Mix 3, and Mix 4 significantly underestimate the ED, which cannot be explained by the experimental or modeling errors. The difference amounts to about 370−500 J/g. Additionally to the pyrolysis ED, the model calculates an ED for sand heating. These model results of the required energy for sand heating to 500 °C account for 471 J/g_{Sand} and are therefore similar to the experimental results (460−490 J/g_{Sand}). Thus, excellent accordance of the experimentally determined and modeled background ED for the reactor, flush gas, and carrier material heating is proven. Sand heating is well calculated compared to the experimental results. The model resolves the allocation of different pyrolysis phenomena that occur during polymer pyrolysis. The sensible heat is indicated as a dominant endothermic share. The heat of the melt accounts for up to 57% of the pyrolysis enthalpy. Because PS does not exhibit a melting point, solid heating is decisive for its pyrolysis ED. The combined reaction and evaporation enthalpy is comparatively low at 23−46%.

The contribution of each polymer in the mixture to the pyrolysis ED is shown in Figure 5. Beyond their impact due to their high content in the mixture, the LDPE and HDPE contribute comparably higher values compared to other polymers as a result of their high heat capacity and heat of fusion. In contrast, PET has a lower melt and reaction enthalpy. The contribution of PET is therefore lower than its proportion in the mixtures. However, the material data are of similar magnitudes and only differ slightly for all investigated polymers. As a result, the mixture's polymer-specific ED correlates strongly with its polymer content.

The additional ED for heating up the sand and the flush gas in the presented pilot-scale pyrolysis is disadvantageous. With a sand-to-feedstock ratio of 4:1 the minimal ED for pyrolyzing the polymers increases by about 1800−2000 J/$g_{Polymer}$. Also, the reaction-related ED is low compared to the heating of the polymer to degradation temperature, which indicates potential opportunities for pyrolysis optimization to enhance the process efficiency. The carrier material should be minimized, and the effective heat recovery from hot products and sand should be implemented in comparable pyrolysis technologies. Also, a more efficient technology for preheating the polymer, e.g., in an extruder, may result in a more sustainable pyrolysis process.

The model predicts the energy requirement of Mixes 2−4 with less precision than that for the other feedstocks. The assumption of the PVC heating behavior is a potential source of this systematical underestimation. However, the PVC content in these mixtures is of max. 5 mol %. Therefore, the PVC material data cannot justify the significant difference between model calculations and experiments. The reason for the underestimation might be found in the model assumption itself. In thermoplastic mixtures, potential interactions occur during the degradation reaction. Degradation mechanisms that differ from pure plastic possibly might lead to a significant difference in the required ED depending on the types of reactions. For example, increased coke formation is observed in thermoplastic blends of polyolefins or PS with PVC or aromatic-containing polymers like PET.[24,28] A systematic investigation of the degradation mechanisms and potential interactions in thermoplastic mixtures will thus be necessary to clarify the cause of the deviations.

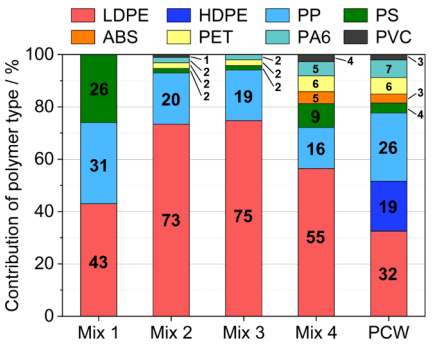

Figure 5. Calculated ED for pyrolysis of the model mixtures Mix 1−4 and die PCW specified by the contributing polymer type.

CONCLUSION

The model presented in this work enables ED calculation of the thermoplastics pyrolysis. The model results are validated in a pilot-scale screw reactor. The total ED for pyrolyzing the plastics is on the order of magnitude of 5% of the net calorific value of the polymeric feedstock, which is about 1575−2424 J/$g_{Polymer}$. The heating of the carrier material requires additional energy. As proven with pure substances or simple mixtures, a high agreement between the model and pilot-scale data is achieved. A systematic underestimation of the experimental data by the model predictions is evident when pyrolyzing heteroatom-containing polymer mixtures. The underestimation of the ED for pyrolyzing more complex mixtures by the model might be attributed to interactions of the polymers during the reaction. Additionally, the model provides detailed insight into dominant endothermic phenomena occurring in the pyrolysis process. The heating of the plastic and the carrier material are the main contributors to the ED.

Detailed investigations are required to better understand potential thermoplastic interactions, which may lead to differing degradation kinetics. The underestimation of the pyrolysis energy requirement is compensated for by this PCW by the present ash content and possible additives, which lower the ED. The transferability of the model based on the material data of additive-free polymers is validated by applying it to the pyrolysis of real PCW. The proven applicability to material systems comprising LDPE, HDPE, PP, PS, ABS, PET, PA6, and PVC enables the approximate calculation of the ED for future reactor designs or pyrolysis system evaluations. In the evaluation of such pyrolytic chemical recycling concepts, further energy requirements must be examined because the ED calculation of this work only covers the physical and chemical aspects of the thermochemical conversion process. For example, the energy required for heat losses, up- and downstream processes, and additional potential material pretreatment, e.g., shredding of the polymeric feedstock, needs to be considered. Depending on the reactor technology used, the ED contribution for reactor-specific accompanying materials must be calculated in the adaption to the pyrolysis system under evaluation.

ASSOCIATED CONTENT

Supporting Information

The Supporting Information is available free of charge at https://pubs.acs.org/doi/10.1021/acssusresmgt.4c00109.

Comparison of the detailed ED results in "experimental results of pilot-scale pyrolysis and model validation", more information about the reactor setup and parameters given in "technical details of the screw reactor", and sensitivity study's in-depth results about the model reaction temperature selection provided in "sensitivity study on the parameter selection for model reaction temperature" (PDF)

AUTHOR INFORMATION

Corresponding Authors

Niklas Netsch − *Institute for Technical Chemistry, Karlsruhe Institute of Technology (KIT), Karlsruhe, Baden-Württemberg 76131, Germany;* orcid.org/0000-0002-2982-181X; Phone: +49 721 608 22869; Email: Niklas.Netsch@kit.edu

Salar Tavakkol − *Institute for Technical Chemistry, Karlsruhe Institute of Technology (KIT), Karlsruhe, Baden-Württemberg 76131, Germany;* orcid.org/0000-0001-5142-2439; Phone: +49 721 608 22898; Email: Salar.Tavakkol@kit.edu

Authors

Michael Zeller − *Institute for Technical Chemistry, Karlsruhe Institute of Technology (KIT), Karlsruhe, Baden-Württemberg 76131, Germany*

Frank Richter − *Institute for Technical Chemistry, Karlsruhe Institute of Technology (KIT), Karlsruhe, Baden-Württemberg 76131, Germany*

Britta Bergfeldt − *Institute for Technical Chemistry, Karlsruhe Institute of Technology (KIT), Karlsruhe, Baden-Württemberg 76131, Germany*

Dieter Stapf − *Institute for Technical Chemistry, Karlsruhe Institute of Technology (KIT), Karlsruhe, Baden-Württemberg 76131, Germany;* orcid.org/0000-0001-6499-062X

Author Contributions

N.N. conceptualized the study, performed the laboratory tests, contributed to the experimental work in pilot scale, and curated the data. H e developed the theoretical model. The writing of the manuscript was performed by him. M.Z. gave support in the conceptualization stage and editing of the manuscript. F.R. contributed to the experimental conceptualization and performed investigations at the pilot scale pyrolysis reactor. B.B. was responsible for the feedstock analysis and reviewed the manuscript. S.T. and D.S. supported the work by supervising, reviewing the manuscript, and acquiring the necessary funding.

Funding

Funding of this work was provided by the German Helmholtz Association within the program "Materials and Technologies for the Energy Transition", under the topic "Resource and Energy Efficiency".

Notes

The authors declare no competing financial interest.

ACKNOWLEDGMENTS

The authors thank Judith Jung from the Institute for Applied Materials of KIT for experimental support in determination of the heat capacities via DSC analyses. We gratefully acknowledge the support of LyondellBasell Industries, INEOS Styrolution, and INEOS Inovyn by providing the polymers.

ABBREVIATIONS

ABS, acrylonitrile butadiene styrene; DSC, differential scanning calorimetry; ED, energy demand; GT, glass transition; HDPE, high-density polyethylene; HHV, higher heating value; LDPE, low-density polyethylene; LHV, lower heating value; PA6, polyamide 6; PCW, post-consumer waste; PE, polyethylene; PET, poly(ethylene terephthalate); PP, polypropylene; PS, polystyrene; PVC, poly(vinyl chloride)

REFERENCES

(1) Lee, R. P. Alternative carbon feedstock for the chemical industry? - Assessing the challenges posed by the human dimension in the carbon transition. *J. Clean. Prod.* **2019**, *219*, 786−796.

(2) Keijer, T.; Bakker, V.; Slootweg, J. C. Circular chemistry to enable a circular economy. *Nat. Chem.* **2019**, *11* (3), 190−195.

(3) European Commission. A European Strategy for Plastics in a Circular Economy. Published January 2018. https://eur-lex.europa.eu/legal-content/EN/TXT/?uri=COM%3A2018%3A28%3AFIN (accessed 2023-12-08).

(4) United States Environmental Protection Agency. National Recycling Strategy. Published November 2021. https://www.epa.gov/system/files/documents/2021-11/final-national-recycling-strategy.pdf (accessed 2023-12-08).

(5) Ministry of the Environment, Government of Japan. Act of Promotion of Resource Circulation for Plastics. Published April 2022. https://www.env.go.jp/en/focus/jeq/issue/vol29/The%20Plastic%20Resource%20Circulation%20Act_0128%20final.pdf (accessed 2023-12-08).

(6) Canadian Council of Ministers of the Environment. Canada-wide Action Plan on Zero Plastic Waste. Published November 2019. https://ccme.ca/en/res/1589_ccmecanada-wideactionplanonzeroplasticwaste_en-secured.pdf (accessed 2023-12-08).

(7) Department of Agriculture, Water and the Environment, Australian Government. National Plastics Plan 2021. Updated October 2021. https://www.dcceew.gov.au/sites/default/files/documents/national-plastics-plan-2021.pdf (accessed 2023-12-08).

(8) Ragaert, K.; Delva, L.; Van Geem, K. Mechanical and chemical recycling of solid plastic waste. *Waste Manage.* **2017**, *69*, 24−58.

(9) Quicker, P.; Seitz, M.; Vogel, J. Chemical Recycling: A critical assessment of potential process approaches. *Waste Manage. Res.* **2022**, *40* (10), 1494−1504.

(10) Agarwal, G.; Lattimer, B. Method for measuring the standard heat of decomposition of materials. *Thermochim. Acta* **2012**, *545*, 34−47.

(11) Cafiero, L.; Fabbri, D.; Trinca, E.; Tuffi, R.; Vecchio Ciprioti, S. Thermal and spectroscopic /TG/DSC-FTIR) characterization of mixed plastics for materials and energy recovery under pyrolytic conditions. *J. Therm. Anal. Calorim.* **2015**, *121* (3), 1111−1119.

(12) Duque, J. V. F.; Martins, M. F.; Debenest, G.; Orlando, M. T. The influence of the recycling stress history on LDPE waste pyrolysis. *Polym. Test.* **2020**, *86*, 106460.

(13) Frederick, W.; Mentzer, C. C. Determination of heats of volatilization for polymers by differential scanning calorimetry. *J. Appl. Polym. Sci.* **1975**, *19* (7), 1799−1804.

(14) Khedri, S.; Elyasi, S. Determination of the heat of pyrolysis of HDPE via isothermal differential scanning calorimetry. *J. Therm. Anal. Calorim.* **2018**, *131* (2), 1509−1515.

(15) Stoliarov, S. I.; Walters, R. N. Determination of the heats of gasification of polymers using differential scanning calorimetry. *Polym. Degrad. Stab.* **2008**, *93* (2), 422−427.

(16) Zeller, M.; Netsch, N.; Richter, F.; Leibold, H.; Stapf, D. Chemical Recycling of Mixed Plastic Wastes by Pyrolysis - Pilot Scale Investigations. *Chem. Ing. Technol.* **2021**, *93* (11), 1763−1770.

(17) Straka, P.; Bičáková, O.; Šupová, M. Thermal conversion of polyolefins/polystyrene ternary mixtures: Kinetics and pyrolysis on laboratory and commercial scales. *J. Anal. Appl. Pyrolyis* **2017**, *128*, 196−207.

(18) Faraca, G.; Astrup, T. Plastic waste from recycling centers: Characterisation and evaluation of plastic recyclability. *Waste Manage.* **2019**, *95*, 388−398.

(19) European Commission. Establishing the identification system for packaging materials pursuant to European Parliament and Council Directive 94/62/EC on Packaging and packaging waste. Published January 1997. https://eur-lex.europa.eu/eli/dec/1997/129/oj (accessed 2023-12-08).

(20) *Thermal analysis—Differential thermal analysis (DTA) and differential scanning calorimetry (DSC)—general principles*; Deutsches Institut für Normung: Berlin, 2019; DIN 51007.

(21) *Plastics—Differential scanning calorimetry (DSC)*; Deutsches Institut für Normung: Berlin, 2023; DIN EN ISO 11357.

(22) Svoboda, R.; Málek, J. Importance of proper baseline identification for the subsequent kinetic analysis of derivative kinetic data. *J. Therm. Anal. Calorim.* **2016**, *124* (3), 1717−1725.

(23) Netsch, N.; Simons, M.; Feil, A.; Leibold, H.; Richter, F.; Slama, J.; Yogish, S. P.; Greiff, K.; Stapf, D. Recycling of polystyrene-based external-thermal insulation composite systems - Application of combined mechanical and chemical recycling. *Waste Manage.* **2022**, *150*, 141−150.

(24) Netsch, N.; Vogt, J.; Richter, F.; Straczewski, G.; Mannebach, G.; Fraaije, V.; Tavakkol, S.; Mihan, S.; Stapf, D. Chemical Recycling of Polyolefinic Waste to Light Olefins by Catalytic Pyrolysis. *Chem. Ing. Technol.* **2023**, *95* (8), 1305−1313.

(25) Netsch, N.; Schröder, L.; Zeller, M.; Neugber, I.; Merz, D.; Klein, C. O.; Tavakkol, S.; Stapf, D. Thermogravimetric Study on Thermal Degradation Kinetics and Polymer Interactions in Mixed Thermoplastics. *SSRN* **2024**. DOI: 10.2139/ssrn.4757121.

(26) Brandrup, J.; Immergut, E. H.; Grulke, E. A. *Polymer Handbook*, 4th ed.; Wiley Interscience Publication, 1999.

(27) VDI Gesellschaft Verfahrenstechnik und Chemieingenieurwesen. *VDI Heat Atlas*, 11th ed.; Springer Vieweg, 2013. DOI: 10.1007/978-3-540-77877-6.

(28) Yu, J.; Sun, L.; Ma, C.; Qiao, Y.; Yao, H. Thermal degradation of PVC: A Review. *Waste Manage.* **2016**, *48*, 300−314.